Improved Cycle Control and Sizing Scheme for Wind Energy Storage System Based on Multi-objective Optimization

Feng Zhang, *Member*, *IEEE*, Guibin Wang, *Member*, *IEEE*, Ke Meng, *Member*, *IEEE*, Junhua Zhao, *Member*, *IEEE*, Zhao Xu, *Senior Member*, *IEEE*, Zhaoyang Dong, *Fellow*, *IEEE*, and Jun Liang

***Abstract*—This paper proposes an improved control and sizing scheme for wind energy storage system for wind smoothing. Considering the trading rules in the electricity market, a cycle control strategy with progressive cycle period including one charge and discharge period is proposed. To determine the reference output and time duration of each cycle control period, a multi-objective optimization model is presented considering both the maximum of time duration of each cycle control period and the minimum of power variation between adjacent charge and discharge intervals. In the proposed control strategy, wind power is smoothed with flexible reference output and self-adjustable battery state of charge (SOC) ranges, and then the battery can be utilized without over-discharge. Meanwhile, the smoothed wind power with longer average interval duration can better benefit the wind power trading in electricity market. Besides, the charge/ discharge switch can be significantly decreased to prolong the battery lifetime. Afterwards, based on the presented control strategy, the sizing methodology is proposed according to the cumulative probability function of the charge/discharge power and energy. Moreover, the impact of wind power forecast error is also considered in the real-time operation. By using actual wind power data, case studies are fulfilled to validate the performance of the proposed cycle control and sizing strategy.**

***Index Terms*—Energy storage system, control, wind power, size**

I. Introduction

WIND energy has been widely deployed in recent years owning to its distinguished features like inexhaustibility and zero-emission [1]. However, due to its stochastic nature, wind energy has brought great challenge to power system operation [2]. Along with the increasing penetration of wind energy, combined with the impacts from the growing demand and less availability of traditional fossil fuel based power resource, wind power system will bring more potential risks to the operation of modern power system [3]. Therefore, the stochastic nature of wind power generation needs to be mitigated to minimize its impacts on system security. Compared with other technologies, energy storage system (ESS) has been considered as the highest potential for wind smoothing [4]. Indeed, with advanced control strategies, ESSs have shown satisfactory performance in mitigating the fluctuation of renewable power generation [5].

In the last decade, researchers have paid much attention to the control strategies of wind energy storage system. A dual-layer control strategy for battery energy storage system (BESS) was presented to mitigate wind power fluctuation in [6]. An optimal control strategy was proposed in [7] to prevent over-charging or deep-discharging of superconducting magnetic ESS through SOC adjustment based on fuzzy logic control theory. Generally the fluctuation of wind generation can be mitigated to a certain degree in the aforementioned literatures. However, it should be noted that there is no specific reference power to demonstrate the smoothing target. In contrast, in other studies, wind power is smoothed with a reference power formulated as a staircase function on hourly basis. A BESS-based operational dispatch scheme for a wind farm was proposed in [8] to reduce the impacts of wind power forecasting error and accordingly determine the optimal battery energy storage system (BESS) capacity. In [9] sizing and control methodologies were presented to smooth the variability of wind power and an artificial neural network was introduced in control strategy to reduce the total cost. In [10], an open-loop optimal control scheme for BESS was proposed to improve the performance of application. Overall, the wind power outputs in the mentioned literatures are on an hourly basis. In fact, the wind power output with fixed time intervals, e.g. hourly, has not been considered in the SOC conditions. If the SOC has spare capacity to release/store wind energy, the time intervals can be prolonged rather than one fixed hour. In this way, the unused capacity can contribute to prolonging time durations to make wind power

This work is supported in part by the National Natural Science Foundation of China under Grant 51307101, 71401017 and 51507103, in part by Natural Science Foundation of Guangdong Province (No. 2015A030310316), in part by Shenzhen University Research and Development Startup Fund (No. 201530), and in part by the 2015 Science and Technology Project of China Southern Power Grid (WYKJ00000027).

F. Zhang and J. Liang are with the Key Laboratory of Power System Intelligent Dispatch and Control, Ministry of Education, Shandong University, Jinan, 250061, China (e-mail: fengzhang@sdu.edu.cn).

G.B. Wang is with the College of Mechatronics and Control Engineering, Shenzhen University, Shenzhen, 518060, China (e-mail: wgbzju@gmail.com).

K. Meng and Z.Y. Dong are with the School of Electrical and Information Engineering, The University of Sydney, Sydney, NSW 2006, Australia; Z.Y. Dong is also with the Electric Power Research Institute, CSG, Guangzhou, 510080, China (e-mail: kemeng@ieee.org, joe.dong@sydney.edu.au)

J.H. Zhao is with the School of Science and Engineering, The Chinese University of Hong Kong, Shenzhen, China.

Z. Xu is with the Department of Electrical Engineering, The Hong Kong Polytechnic University, Hong Kong, China.

become more dispatchable, improving the feasibility and flexibility of the market trading.

Currently, since ESS is still a non-cheap option to address wind power fluctuation, prolonging its lifetime should be taken into consideration in the process of ESS planning and real-time operation [11]. Moreover, over-discharge is regarded as one of the most serious issue of BESS, e.g. lead-acid battery [12]. For this reason, a number of possible solutions have been proposed. An improved sizing method for a wind-solar-battery system was presented in [13], where the battery's depth of discharge (DOD), charge/discharge current, rate and cycles to prolong BESS lifetime were considered in BESS control strategy. To mitigate the risk during electricity trading, an optimal sizing and allocation method was proposed in [14] through a cost-benefit analysis model, in which minimum SOC was set to protect BESS. A conventional feedback-based control scheme proposed in [15], where the SOC was kept within a certain range to achieve best utilization of BESS. In these studies, BESS is protected through a set of fixed SOC limits. However, if the limit lines are too high or too low, it will bring a waste of energy capacity or potential damages to the battery [16]. Besides, research on the relationship between discharge power and the usable energy capacity in [12] shows that when the battery discharges with a higher power than the rated value, the total energy capacity will decrease rather than keep constant as the rated value. For example, the BESS, e.g., (1MW, 4MWh), discharges with 1.3MW that is higher than the rated value (1MW), then the total usable energy capacity is not 4MWh but smaller. However, the nonlinear relationship between discharge power and the usable energy capacity has not been considered in the simulation of traditional BESS control strategies. In such case, although SOC seems to be within the allowable range in the simulation, actually over-discharge has already occurred. Furthermore, from another aspect, the frequent switching between charge/discharge modes can shorten the battery life span [17], which also needs to be considered in the control strategy design.

As a result, an improved cycle control and sizing strategy for BESS is proposed in this paper. During each control period, the lead-acid BESS charges and discharges once, and accordingly SOC varies from a peak value to a valley value. Meanwhile, flexible upper and lower ranges are introduced to constrain SOC and guarantee the utilization of the battery. During the determination of the range boundaries, the nonlinear model between discharge power and usable energy capacity is considered. Moreover, according to the SOC conditions, the time duration of each interval is determined to be N (N=1, 2…) times of the trading period (dispatch interval) in the electricity market, e.g. half an hour [18]. Afterwards, a multi-objective model attempting to maximize the cycle control duration and minimize the power variation between the adjacent charge and discharge interval is proposed to determine each charge/discharge interval and reference power output. Subsequently the power capacity and energy capacity of the lead-acid battery are sized by a cumulative probability function of the charge/discharge power and energy. Furthermore, the real-time operation of the lead-acid battery is also discussed mainly considering the impacts of wind power forecast error.

The rest of this paper is organized as follows. The charge/discharge cycle control rules are introduced in Section II; the multi-objective optimization model for cycle control strategy is proposed in Section III; capacity determination method based on the presented cycle control strategy is described in Section IV; the real-time operation of BESS is discussed in Section V; case studies are given in Section VI; and the conclusion is drawn in Section VII.

II. The Proposed Cycle Control Strategy

Lead-acid battery is regarded as suitable for mitigating renewable energy fluctuations due to its mature technique and low cost [19]. Compared with other technologies, lead-acid battery has been widely used over several decades. More importantly, lead-acid battery is most economical in terms of cost of about 300 $/kWh, which is much lower than other electrochemical batteries. Consequently considering the huge capital investment requirement of grid-scale ESS, nowadays lead-acid battery is still a competitive technology. In this proposed control strategy, the main goals are achieving better technical and economical performances of the lead-acid BESS. Specifically, the proposed control strategy with flexible reference output and SOC ranges can effectively avoid over-discharge and decrease charge/discharge switch to prolong the battery lifetime. Meanwhile the smoothed wind power with prolonged interval durations can benefit the wind power trading in electricity market.

A. Charge/discharge Cycle Control Rules

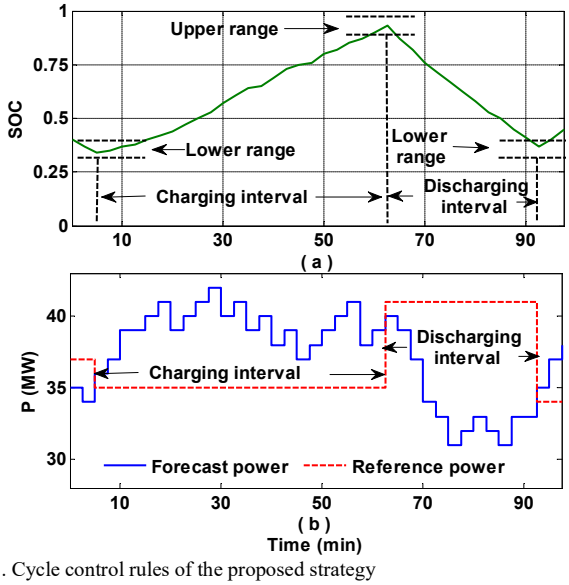

Fig.1. Cycle control rules of the proposed strategy

As shown in Fig.1 (a), each cycle control period includes one charge and discharge interval with flexible time duration. During the charge interval, the battery keeps charging from the initial value that is within the lower range until SOC reaches the upper range. Afterwards, the battery switches to discharge and SOC decreases in a monotonous manner into the lower range.

Specifically, as shown in in Fig.1 (b), the charge/discharge control logic is set as follows.

Charging strategy for BESS:

$$P_t^w > P_t^r \tag{1}$$

$$P_t^c = P_t^w - P_t^r \tag{2}$$

$$C \cdot \left| SOC_{c0} - SOC_c \right| = \eta^c \cdot \sum_{t=t_{c0}}^{t_c} P_t^c \cdot t \tag{3}$$

where P_t^w is the wind power; P_t^r is the reference power; P_t^c is the charge power; C is the rated energy capacity of BESS; SOC_{c0} and SOC_c are the initial and terminal SOC values during the charge interval; and $SOC_h^L \geq SOC_{c0} \geq SOC_l^L$, $SOC_h^U \geq SOC_c \geq SOC_l^U$, $[SOC_l^U, SOC_h^U]$, $[SOC_l^L, SOC_h^L]$ are SOC upper and lower ranges, respectively. $[t_{c0}, t_c]$ is the charge interval. η^c is the charge efficiency.

Discharging strategy for BESS:

$$P_t^w < P_t^r \tag{4}$$

$$P_t^d = P_t^w - P_t^r \tag{5}$$

$$C \cdot \left| SOC_{d0} - SOC_d \right| = \frac{1}{\eta^d} \cdot \sum_{t=t_{d0}}^{t_d} -P_t^d \cdot t \tag{6}$$

where P_t^d is the discharge power; SOC_{d0} and SOC_d are the initial and terminal values, and $SOC_h^U \geq SOC_{d0} \geq SOC_l^U$, $SOC_h^L \geq SOC_d \geq SOC_l^L$. $[t_{d0}, t_d]$ is the discharge interval. η^d shows the discharge efficiency.

Among traditional micro-cycle control strategies, e.g. hourly interval, the reference power is calculated as the average value of hourly wind power. Apparently it is prone to incur over-discharge and frequent charge/discharge switch. Consequently, the advantages of the proposed control strategy with flexible reference output can be summarized as follows:

1) Monotonous charge/discharge enables BESS store and release relatively more energy in each charge/discharge interval. It guarantees the effectiveness of fluctuation smoothing and makes it possible to prolong the charge/discharge interval duration to benefit wind power trading.

2) The flexible reference output can effectively constrain the charge/discharge power and avoid over-discharge.

3) The frequency of charge/discharge mode switch can also be decreased to avoid the potential damage to BESS.

B. Flexible SOC Ranges

The tradeoff between the utilization efficiency and potential damage to batteries needs to be considered when determining SOC ranges. The utilization may be promoted by the inappropriate lower range, but over-discharge is also prone to occur. Consequently, according to the limit settings in [13-15], $[SOC_l^U, SOC_h^U]$ and $[SOC_l^L, SOC_h^L]$ in this study are preliminarily determined to be [0.85,0.95] and [0.25,0.35], respectively.

However, such settings are based on the rated power capacity. In fact, BESS has an ability of high rate discharge, which means the battery can discharge with a higher power than the rated value which may occur quite often when wind power fluctuates dramatically [12]. However, the negative effect of the high rate discharge is that the usable energy capacity of BESS will be decreased and formulated as a nonlinear and decreasing function of the discharge power. According to the experimental data in [12], least square method based curve fitting function is built in this study. Fig.2 shows the fitting curve in which the discharge power and energy capacity are the per unit values of the rated power capacity and rated energy capacity, respectively.

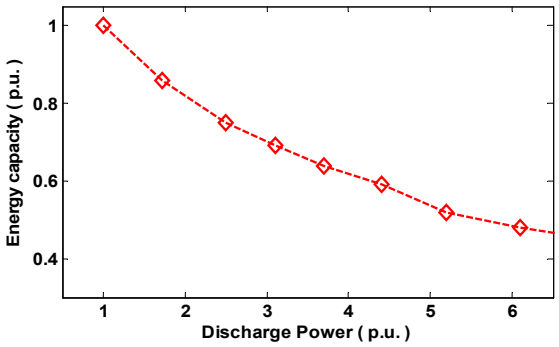

Fig.2. Relationship between the energy capacity and the discharge power

It can be observed that if BESS discharges with a higher rate value, the usable energy capacity decreases accordingly. Normally when the usable energy capacity is 1, i.e., the x and y axis are both 1, the maximum energy E that can be released in the discharge interval is computed as

$$E = C \cdot (SOC_h^U - SOC_l^L) \tag{7}$$

Then SOC_l^L can be calculated by the following transformation:

$$SOC_l^L = SOC_h^U - E/C \tag{8}$$

However, when the usable capacity decreases to be C′ (C′ < C) , and assuming that in simulation this factor has not be considered in the battery management system (BMS), BESS will still release energy with the maximal energy limit E, then

$$SOC_l^L{}' = SOC_h^U - E/C' \tag{9}$$

where $SOC_l^L{}'$ is the actual SOC value. Obviously, $SOC_l^L{}' < SOC_l^L$, which means over-discharge has already occurred in such case. Consequently, in order to avoid this situation, SOC_l^L and SOC_h^L have to be adjusted timely as follows when BESS releases energy with high-rated discharge:

$$SOC_l^L{}'' = SOC_h^U - (SOC_h^U - SOC_l^L) \cdot C' / C \tag{10}$$

$$SOC_h^L{}'' = SOC_l^L{}'' + (SOC_h^U - SOC_l^L) \cdot C' / C \tag{11}$$

where $SOC_l^L{}''$, $SOC_h^L{}''$ are the new boundaries of lower range. C' is formulated as a function of discharge power P_t^d, i.e., $C'=F(P_t^d)$. This function may be slightly different because the batteries of different manufactures may not show the exactly same characteristics, but the functions show similar trends. In this study, the curving fitting function in Fig.2 is adopted for the calculation of C'. Specifically, with the aim of protecting BESS, the SOC lower range will be adjusted as long as the instantaneous discharge power is larger than the rated value in the discharge interval in this research.

C. Battery Lifetime Model

Given the complicated ageing process, it is not easy to accurately model the battery lifetime [20]. Generally the factors such as temperature, usage pattern and degradation mainly

affect the battery lifetime. Accordingly, researches on battery lifetime model have been conducted to predict the remaining battery lifetime [21]. Among others, the method based on total energy throughput is relatively easy to be implemented, in which normally the total charge/discharge energy during the whole battery lifespan is treated as constant [14]. The lifetime of battery can be calculated as

$$L = T \cdot \frac{Cyc_r \cdot D_r \cdot C}{\sum_{i=1}^{m} E_i} \tag{12}$$

where L is the battery lifetime. Cyc_r is the life cycles at certain DOD D_r. m is the total number of discharge intervals during a certain time period T. E_i is the discharging energy of the i^{th} interval.

$$E_i = w_i^o \cdot D_i \cdot C \tag{13}$$

where D_i is the DOD of the i^{th} discharge interval. w_i^o is the penalty coefficient to demonstrate the potential damage of over-discharge. When over-discharge occurs, w_i^o will be larger than 1 aiming to quantify the damage by equivalently enlarging the energy consumption, otherwise w_i^o will be constant as 1.

It should be noted that for simplicity other factors such as temperature and charge/discharge switch have not been included in the presented models. In fact, generally the prevailing energy storage stations are built indoors to maintain the temperature within proper ranges. Meanwhile, the frequent charge/discharge switch can affect the chemical reaction process, and obviously the decrease of charge/discharge switch can benefit the battery lifetime.

III. Optimal Cycle Control Based on Multi-objective Model

Based on the proposed control strategy, an optimal cycle control model is presented in this research, which can be implemented progressively. The charge/discharge interval duration of each cycle control in this paper promotes the quality of the reference wind power. Besides, the power ramp of adjacent charge/discharge intervals is taken into consideration to constrain the overall variation of the reference output.

A. Charge/discharge Interval Duration

Charge/discharge interval duration of each cycle control period is not predetermined as traditional methods, but computed under the proposed optimal cycle control model in this study. Obviously the longer intervals result in higher dispatch-ability of wind power, which can participate in market bidding of longer time horizons. Moreover, the longtime intervals can significantly decrease the total times of the charge/discharge mode switch over a certain period, e.g. one year, to greatly prolong the life span of battery. For this purpose, considering the trading rules in electricity market, the charge/discharge interval duration is constrained to be N times of the electricity trading period. The i^{th} charge/discharge interval can be expressed as

$$t_i^c = N^c \cdot \Delta t \tag{14}$$

$$t_i^d = N^d \cdot \Delta t \tag{15}$$

where Δt is the electricity trading period. t_i^c and t_i^d are the charge and discharge interval duration of the i^{th} control period, respectively. N^c and N^d are positive integers. In this study, Δt is 0.5 hour according to the market rules in [18].

B. Power Ramp of Adjacent Charge/discharge Intervals

During the cycle control period, since the charge and discharge energy are constrained, the reference power and the corresponding interval duration are mutually constrained. If the optimization target only focuses on the maximization of interval duration, the power ramp of the adjacent charge/discharge intervals may become much larger. Hence, as shown in Fig.1(b), the power ramp of adjacent charge and discharge intervals need to be considered. Furthermore, the constraints of power ramp benefit the market bidding as well.

C. Multi-objective cycle control model

In this study, by maximizing each control period duration and minimizing the ramp rates of reference output, the charge/discharge interval duration and reference output are optimally calculated.

1) Maximization of each control period duration: With the aim of prolonging each control period, the model for the i^{th} (i=1, 2, 3…) control interval is built as

$$\max t_i = t_i^c + t_i^d \tag{16}$$

where t_i is the time duration of the i^{th} control interval.

2) Minimization of the ramping rates of reference output: As shown in Fig.1 (b), the optimization model of the i^{th} ($i \geq 2$) interval is mathematically formulated as a variance function.

$$\min f_i = \frac{1}{i} \cdot \sum_{n=2}^{i} \left\{ \left[\left(P_{n\text{-}1}^{rd} - P_{n-1.n}^{v} \right)^2 + \left(P_n^{rc} - P_{n-1.n}^{v} \right)^2 \right] + \left[\left(P_n^{rc} - P_n^{v} \right)^2 + \left(P_n^{rd} - P_n^{v} \right)^2 \right] \right\} \tag{17}$$

s.t.

$$P_t^c \leq P_t^{cmax} \tag{18}$$

$$|P_t^d| \leq |P_t^{dmax}| \tag{19}$$

$$\left| P_{n\text{-}1}^{rd} - P_n^{rc} \right| \leq P^{rmax} \tag{20}$$

$$\left| P_n^{rc} - P_n^{rd} \right| \leq P^{rmax} \tag{21}$$

where P_{n-1}^{rd} is the reference power of the $(n\text{-}1)^{th}$ discharge interval, P_n^{rc} and P_n^{rd} are the reference power of the n^{th} charge and discharge interval, respectively. $P_{n-1,n}^{v}$ is the average value of P_{n-1}^{rd} and P_n^{rc}, and P_n^{v} is the average value of P_n^{rc} and P_n^{rd}. P_t^{cmax} and P_t^{dmax} are the maximum values of charge and discharge power, P^{rmax} is the maximum value of the ramp rates. Obviously, both the ramp rate in the i^{th} interval and all previous intervals are considered in this paper to constrain the overall variation of the reference output.

D. NSGA II--based Solution Method

Non-dominated sorting genetic algorithm II (NSGA II) is considered efficient for multi-objective optimization [22]. The detailed implementation procedure of NSGA II in this study is as follow.

Step 1) Coding: Real coding strategy is adopted for each individual that is composed by decision variables, i.e. t_i^c, t_i^d, P_i^c, P_i^d, SOC_c and SOC_d.

Step 2) Initialization: The initialization contains BESS operation parameters, e.g. Δt, η^c and η^d, and NGSA II calculation parameters, e.g. population size Z, objective number B , maximum generation G and hyperspace dimension D. The random initialization will be checked whether the parameters are meeting the charge/discharge rules. If not, these parameters need to be reinitialized.

Step 3) Non-dominated sort: After initialization, the objective functions of each individual, i.e., t_i in (16) and f_i in (17), are calculated, and the non-dominated levels of individuals are determined by a fast non-dominated sorting scheme.

Step 4) Crowing distance: If the non-dominated sort is completed, the crowding distance is assigned for every individual in each population in the following manner.

$$d_i = d_i + \frac{d_{i+1}^m - d_{i-1}^m}{d_{\max}^m - d_{\min}^m} \tag{22}$$

where d_{i+1}^m, d_{i-1}^m are the values of the m^{th} objective function of the $(i+1)^{th}$ and $(i-1)^{th}$ individuals; d_{max}^m and d_{min}^m are the maximal and minimal values of the m^{th} objective function in this population. Larger crowing distance will result in better diversity in the population, and meanwhile the comparison between two individuals in different fronts is meaningless.

Step 5) Selection and recombination: The individuals are selected by a tournament selection with crowed comparison operator. After that, elite strategy is adopted to transmit the excellent individuals of a parent generation into an offspring generation. The new generation is filled by each front subsequently until the population size exceeds the current population size. When the iteration reaches maximum generation, NSGA II ends with an output of non-dominated solution.

IV. Probabilistic Model for Capacity Determination Based on the Proposed Cycle Control

Capacity sizing including energy capacity and power capacity can be categorized into BESS planning, which is designed under a specific objective function with historical data over a certain period [23]. Considering the periodic feature of wind power, normally annual power data are used for BESS capacity determination [13].

A. Probabilistic model for capacity determination

According to the optimal cycle control of BESS, energy capacity requirements of each cycle control period are various due to the different time durations and reference power values. Considering the high price of battery per unit size, if BESS is required to meet the energy capacity requirements of all control periods, the rated energy capacity will be too large to be reasonable. For this reason, an approach is presented to achieve the tradeoff between the performance and cost by the cumulative probability function (cpf) of energy capacities of each cycle control period during one whole year.

1) Energy capacity: According to the optimal cycle control strategy, the interval duration, reference power and energy capacity requirement of each control period are progressively computed for one whole year. Consequently, the probability density function (pdf) of energy capacities of one whole year can be statistically calculated. According to the cpf of energy capacity, the rated value is expected to meet capacity requirements with the probability of p ($0< p \leq 1$).

$$P\,(0 \leq C_i \leq C\,) = p \tag{23}$$

where P is the probability function; C_i is the energy capacity of the i^{th} control period. It can be observed that the rated capacity is mainly determined by the selection of p. If p is too low, accordingly the rated energy capacity will be small, and then it may shorten charge/discharge interval duration and increase the power ramp. On the other side, if p is too high, the rated energy can satisfy the charge/discharge requirements, but it will significantly increase the investment cost. For this reason, according to the previous work in [14] and the simulation in this study, p is set as 0.85 aiming to get a reasonable energy capacity.

However, if P_i^{rc}, P_i^{rd}, t_i^c, t_i^d and C_i are all stochastically initialized without any constraints, the calculation burden of annual wind power will be too large. Besides, if the optimization targets only focus on (16) and (17) with no constrains, C^i may be easily increased to an unreasonable value. For this reason, in this research C_i and t_i (sum of t_i^c and t_i^d) are constrained within specific limits to get feasible and quick solution.

a) Constraint of C_i: Research in [15] concludes that an effective smoothing can be achieved if the energy capacity is designed to be 20% - 30% of the wind power capacity, e.g., a 10-15 MWh BESS is integrated within a 50 MW wind farm. With the aim to reduce the calculation burden and guarantee the global optimal solution, only the upper bound is adopted in this research and enlarged to be 50%. Considering the installed capacity of wind farm for simulation in this research, i.e. 36 MW, C_i is constrained within 18 MWh.

b) Constraint of t_i: During the real-time operation of BESS that will be discussed in the next section, wind power forecast error needs to be considered. Normally the forecast error will increase if the forecast time horizon extends. Consequently, with the aim to decrease the impact of forecast error, t_i is assumed to be within the time scale of the very short term forecast, i.e. 3 hours [3].

2) Power capacity: After P_i^{rc}, P_i^{rd} of each control period are determined, cpf of the charge and discharge power of the whole year can also be calculated. Accordingly the rated charge and discharge power can be determined in a similar manner.

$$P\,(0 \leq P_t^c \leq P^c\,) = p^c \tag{24}$$

$$P\,(0 \leq P_t^d \leq P^d\,) = p^d \tag{25}$$

where P^c, P^d are the rated power energy capacity. p^c, p^d are the probabilities for determining the charge and discharge power.

B. Steps for implementation of the presented cycle control and sizing scheme

According to the optimal cycle control rules and the probabilistic model for capacity determination, steps for implementing the proposed methodology are shown in Fig. 3. Due to

the periodic feature of wind power, annual wind power data is used for the calculation.

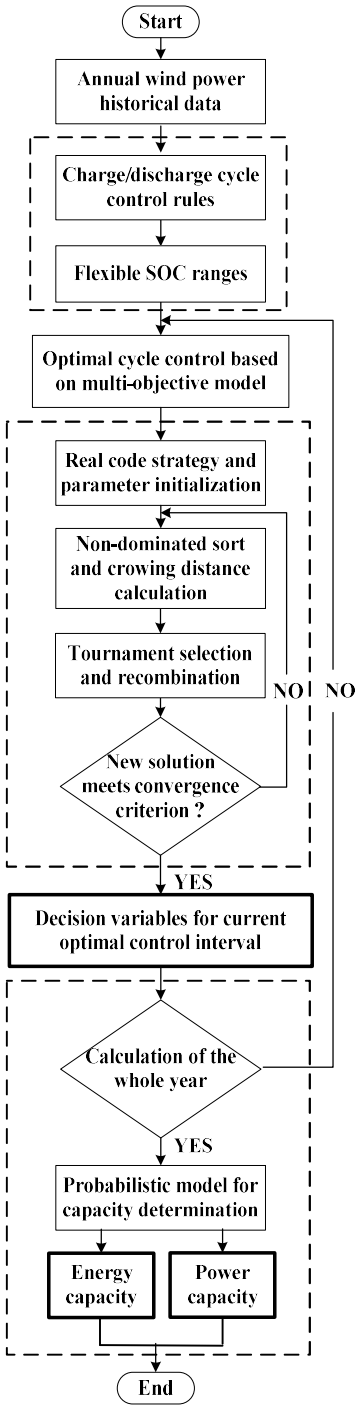

Fig.3. Steps of implementation of the presented strategy

V. Application of the Proposed Methodology in Real-time Operation

After planning the rated capacity, the designed BESS will operate in real-time with the optimal cycle control strategy. In contrast with the capacity planning on basis of historical wind power data, in the real-time operation near-future control parameters of BESS need to be pre-computed. Wind power forecast provides possibility for the upcoming cycle control period [24].

A. Real-time Operation of BESS

It is worth noticing that forecast error of wind power is inevitable. Furthermore, in the prevailing market trading, once the wind power generation schedule is submitted to the transmission system operator (TSO), the schedule adjustment will not be allowed within a predefined hours (say 4 hours) [25]. So if the actual generation differs from the schedule, the wind power plant will take high financial penalty. Consequently, the forecast error needs to be addressed in the real-time operation.

In fact, there are many choices that are suitable for addressing the forecast error, such as ESS or other generation units. It should be noted that forecast error is addressed independently from the lead-acid BESS. For this reason, the structure in Fig.4 shows the proposed control scheme, in which the vanadium redox battery (VRB) is introduced to deal with the forecast error independently from the lead-acid BESS.

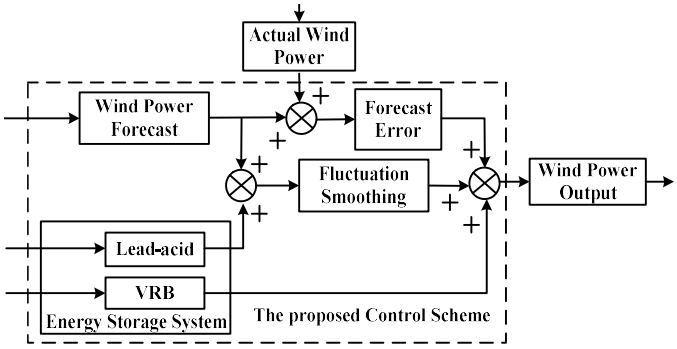

Fig.4. Structure of the proposed control scheme

Since the very short term forecast can reach high precision with an RMSE of 10% [16], the capacity requirements of VRB will not be high, so there is not necessary to concern the increment of investment cost. In fact, forecast error varies frequently with small amplitudes, and VRB is quite appropriate for the forecast error due to its long life span, low maintenance requirements, and especially no constraints on charge/discharge switch [26], so VRB is flexible to track the forecast error. When the forecast is above zero, VRB will charge and the charge power equals the forecast error, otherwise VRB will discharge and the discharge power (negative) also equals the forecast error.

B. Applicability of the Improved Methodology

To demonstrate the applicability of the presented methodology, the framework of this paper is shown in Fig. 5. Generally control strategy of BESS is essential for a wind farm-BESS system both during the process of BESS planning and real-time operation. With the designed control strategy, capacity planning of BESS can be conducted with historical wind power data. Afterwards, based on the control strategy and planned capacity, BESS can operate in real-time application. Capacity planning and real-time operation of BESS require historical and forecast wind power data, which normally can be obtained from the wind power database and wind power forecast system, respec-

tively. Consequently, the presented methodology is adaptable for scenarios in wind farm-BESS systems, and it can guarantee the applicability.

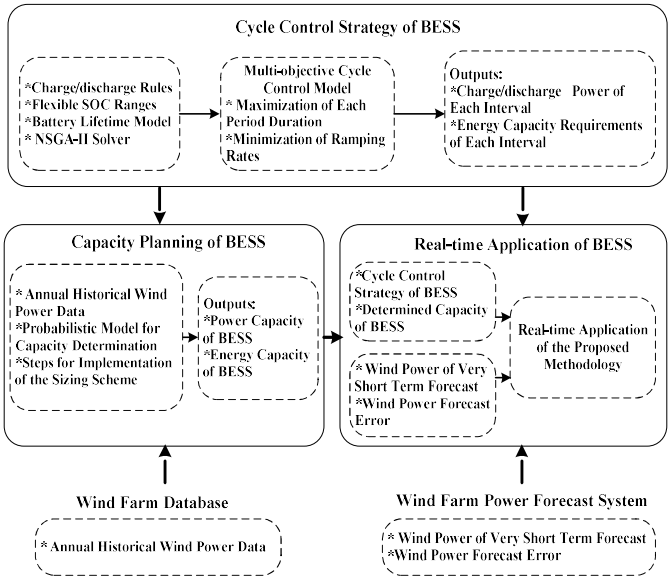

Fig.5. Framework of the presented methodology

VI. Case Study

The presented control and sizing scheme is verified using actual power data from wind farms located on the southeast coast of China. The installed capacity is 36 MW. Table I shows the parameter setting in the case study.

TABLE I
PARAMETER SETTING IN CASE STUDY

BESS operation parameters		
Δt	Electricity trading period	0.5 h
P_t^{cmax}	maximum value of the charge power	5 MW
P_t^{dmax}	maximum value of the discharge power	6 MW
P^{rmax}	maximum value of the ramp rates	18 MW
η^c	Charge efficiency	0.9
η^d	Discharge efficiency	0.95
p	Probability for energy capacity determination	0.85
p^c	Probability for charge power capacity determination	0.95
p^d	Probability for discharge power capacity determination	0.95
NSGA II calculation		
Z	Population size	100
B	Objective number	2
G	Maximum generation	1000
D	Hyperspace dimension	6

A. Evaluation of the Cycle Control Strategy

Performance indexes are defined in this paper as an evaluation scheme to demonstrate the advantages of the cycle control strategy.

1) Total times of charge/discharge mode switch N. N is introduced to evaluate the frequency of charge/discharge mode switch in one whole year. Obviously if N decreases, less damage will be incurred to prolong the lifespan of BESS.

2) Average time duration of charge/discharge intervals t_Δ. t_Δ is computed as dividing the time horizon of the data by the total number of charge and discharge intervals. Obviously, t_Δ can evaluate the dispatch-ability level of the reference output. The longer t_Δ represents higher dispatch-ability of the reference output.

3) Average value of f_i *during one whole year* f. f is calculated by (26) aiming to show the overall variations of ramp rates of the reference output during one whole year.

$$f = \frac{1}{h} \cdot \sum_{i=1}^{h} f_i \tag{26}$$

where h is the total number of control periods during one year. Obviously, since f_i is used to constrain the ramp rate of the i^{th} interval, f shows the overall variation, and the smaller f benefits the wind power dispatch.

Using the annual historical wind power data, the cycle control periods can be progressively calculated, and meanwhile the capacity requirement of each control period can be obtained.

TABLE II
EVALUATION INDEXS

Index	N	t_Δ	F
Hourly reference output	14965	60 min	108
Reference output in this paper	4745	110 min	65

Table II shows the evaluation indexes of the simulation results. In traditional hourly output methods, the hourly reference output value is calculated as the average of wind power within one hour interval. Afterwards, charge/discharge mode is determined by the deviation between the reference output and the wind power, and BESS will charge when the reference is larger than the wind power, otherwise ESS will discharge.

Apparently, Table II shows that the presented control strategy significantly decreases the total times of charge/discharge switch. Correspondingly, the average daily times of the presented strategy are 13, in contrast with 41 times of the hourly reference output. Obviously, the proposed control strategy could effectively avoid the potential damage to BESS.

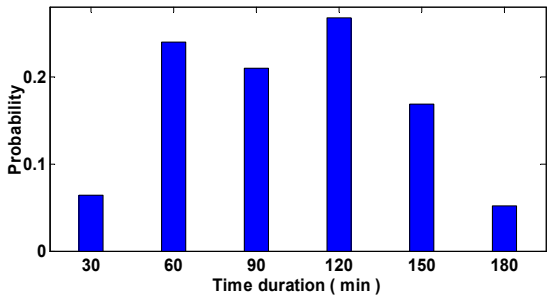

Fig.6 Probability distribution of the interval duration

Subsequently, t_Δ in the proposed strategy is calculated to be 110 minutes, which is much longer than the hourly output. For further demonstration, Fig.6 shows the probability distribution of the annual interval duration. It should be noted that more than 90% of intervals are longer than one hour, and consequently this further verifies the performance of the presented control strategy. Furthermore, f in Table II is much smaller than

the hourly output, which means the overall variations of ramp rates can be effectively constrained in this research.

B. SOC Conditions

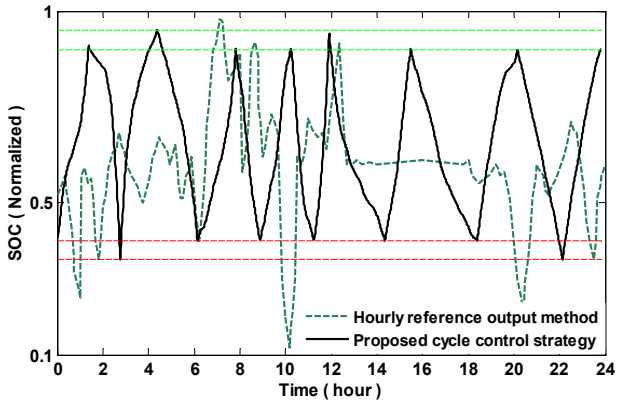

Fig.7 Comparison of SOC conditions

Fig. 7 shows SOC conditions of hourly reference output method and the proposed cycle control strategy. It can be noted that BESS in this research can not only fully utilize the size-limited capacity during each cycle control period, but also effectively avoid over-discharge. Besides, Fig.8 shows that SOC ranges are flexible to make adjustment to avoid potential over-discharge incurred by the high rate discharge.

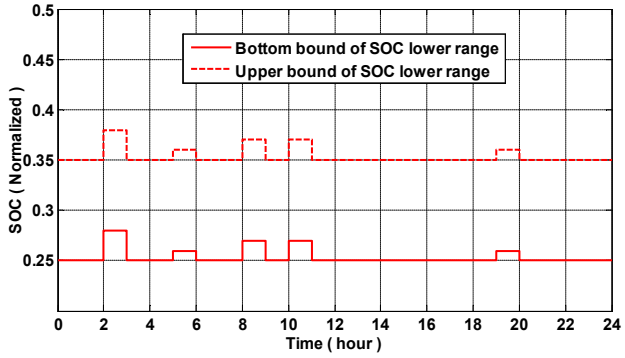

Fig.8 Flexible SOC ranges

Fig.9 shows the reference power determined by the cycle control strategy. Apparently, the reference output can track the fluctuation pattern of the wind power. Besides, the average interval duration is verified to be longer than hourly output, and accordingly improve the dispatch-ability and the trading reliability.

Moreover, considering the seasonal feature of wind power variations, BESS will operate under conditions in various seasons. In Fig.10, four typical days of each season are chosen to show the SOC conditions. Obviously, SOC in mild wind season, e.g., summer, has less charge/discharge switch and longer average time duration, while BESS in winter switches frequently with shortest average interval duration. However, it can be observed that BESS has been fully used in the four seasons. It can be seen that the seasonal pattern of wind power variations have little impact on the presented control strategy.

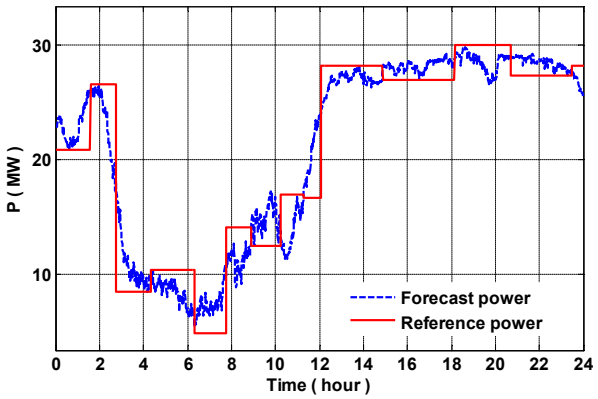

Fig.9 Reference output in this research

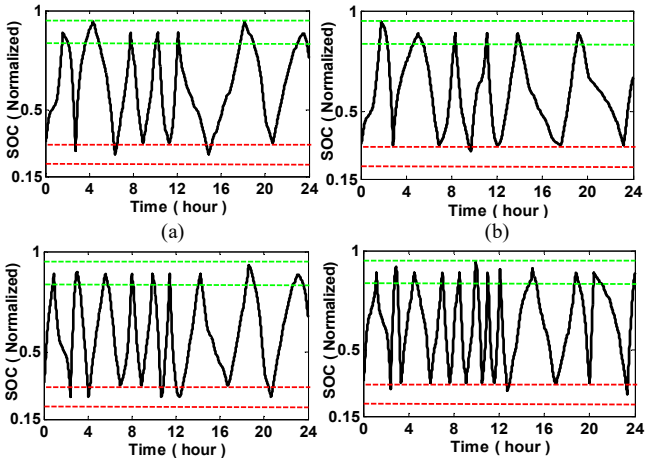

Fig.10 SOC curves of typical days in various seasons. (a) spring; (b) summer; (c) autumn; (d) winter

C. ESS Capacity Determination

By statistically calculating the capacity requirements of the whole year, cpf of the power and energy capacity can be computed and then the rated power and energy capacity can be statistically determined. Fig.11 shows the cpf of P^c, P^d and C_i, respectively. It can be seen that when cpf of C_i equals 0.85, the rated energy capacity is 10.3 MWh accordingly.

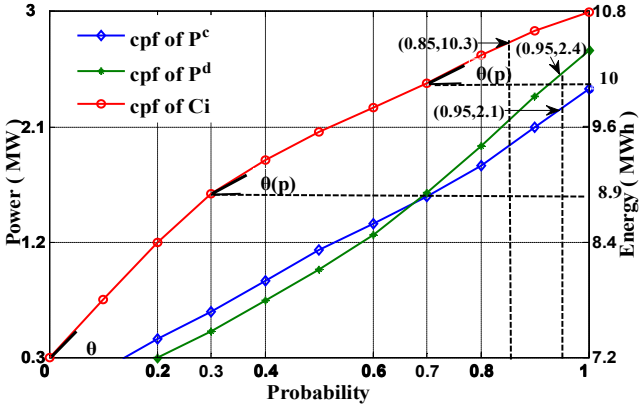

Fig.11. cpf curves of the energy capacity and the charge/discharge power

Furthermore, from the slope of angle $\theta(p)$ of the C_i curve, as shown in Fig. 11 and 12, it can be observed that $\theta(p)$ can be roughly analyzed by three stages divided by the slope values,

which is expressed as the value of the energy capacity variation (y axis) when the probability (x axis) increases per unit value. During the initial stage, i.e., probability values (x axis) are approximately within [0, 0.3], the slope values are high; and in the middle stage [0.3, 0.7], the slope becomes relatively lower; and in the end stage [0.7, 1], the slope arises again.

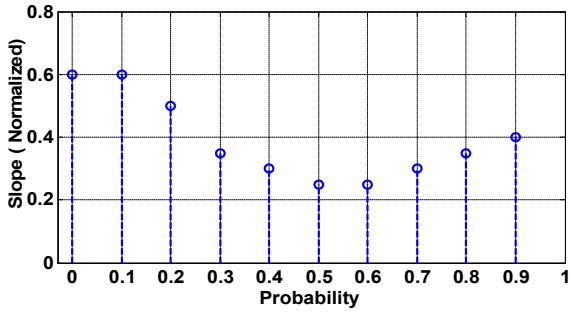

Fig.12. Slope of cpf curve of C_i

Obviously, the high slope means that the same probability increment results in large energy capacity variation. In other words, the probability density of C_i is relatively low in this stage, i.e., [7.2, 8.9] MWh, as shown in Fig.11. Afterwards, the slope decreases in the middle stage, which means that the probability density of C_i increases, so there is a high probability of C_i appearing in this stage [8.9, 10] MWh. In contrast, during the end stage, the slope increases and the probability density of C_i falls again, but the average density is still higher than the initial stage. From the analysis of the probability distribution of C_i, it can be seen that the selection of p value, i.e. 0.85, can cover the area of high probability density and result in a reasonable energy capacity. Consequently, the selection of p is reasonable and it facilitates the tradeoff between the BESS cost and its performance.

Since capacity requirements of the control periods are various while the rated energy capacity is unique, there might be a concern that in the following real-time operation, under the cycle control strategy the energy capacity determined by cpf may not simultaneously satisfy the equation constraints (1) and (2) of all periods. In fact, during the calculation when the capacity requirement is smaller than the rated value, the solution will adjust the reference output, and then the equations can be satisfied to get the feasible value. On the other side, when the capacity requirement is larger than the rated value, the reference output and time duration of each period can be adjusted according to the unused energy capacity to get an optimization solution. There might exist an extreme case that the time duration has been decreased to be half an hour (minimum value), and meanwhile the SOC has reached SOC_h^U or SOC_l^L, which implies there is not sufficient capacity to charge or discharge. Normally, such cases are caused by extreme weather like hurricane. However this is actually a fairly rare occurrence. If it happens, Δt can be adjusted to be smaller, e.g. 15 min, to get a solution for such a special case. Actually such case does not occur during this research.

Subsequently, according to the cpf of P^c and P^d in Fig. 11, it can be observed that the rated charge and discharge power are determined as 2.1 MW and 2.4 MW respectively.

To fully validate the performance of the cycle control and sizing scheme, capacity requirements of different control strategies are used to verify whether the presented strategy can decrease the BESS capacity. To establish the basis for comparison, several index parameters are introduced to guarantee that the fluctuation smoothing performances are at a similar level. Besides, three cases with same average interval duration have been proposed. In Case 1 and 2, the reference power is calculated as the average value of the wind power of predetermined interval progressively, i.e. 110 minutes. In Case 3, the reference power is determined by the proposed multi-objective optimization.

TABLE III
COMPARISON OF CAPACITY REQUIREMENTS

	Case 1	Case 2	Case 3
Average time interval duration	110 mins	110 mins	110 mins
E_{dev} (MWh)	837	869	769
N	12784	12784	4745
Over-discharge	Not constrained	SOC range [0.15,1]	Flexible SOC ranges
Charge/discharge power capacity	4.7/5.4 MW	4.7/5.4 MW	2.1/2.4 MW
Energy capacity	13.6 MWh	14.7 MWh	10.3 MWh

Table III shows simulation results with annual wind power data. E_{dev} shows the power deviation between the reference output and the smoothed wind power to demonstrate the performance of fluctuation smoothing, and N is still used to show the frequency of charge/discharge switch. It can be seen that when similar average interval duration and fluctuation smoothing performance have been achieved, the power capacity and energy capacity in Case 1 and 2 are both larger than that in Case 3. Specifically, the charge/discharge power in Case 1 and 2 is 4.7/5.4 MW. The reason is that reference power in Case 1 and 2 is progressively calculated as the average value of the wind power of predetermined interval, while the reference power in Case 3 is optimized with the proposed multi-objective model. Consequently, the power capacity requirement is higher than Case 3. Subsequently, compared with Case 1 and 2, the energy capacity in Case 3 has been significantly decreased with the presented control and sizing scheme.

From the analysis above, it can be seen that the proposed cycle control and sizing scheme in this paper can significantly decrease the power capacity and energy capacity of BESS. Besides the capacity reduction, in Table III it should be noted that the proposed strategy in Case 3 can provide better protection to BESS by decreasing N and effectively avoiding over-discharge.

D. Performance of the Real-time Operation

Considering the precision of very short term forecast, the capacity requirement of VRB is much lower than the lead-acid BESS, and a 1MWh/2MW VRB system is selected according to the statistical calculation of forecast error. Fig.13 shows the smoothing effectiveness of wind power, which includes the

comparisons between the forecast power, actual wind power, reference power and the actual smoothed power.

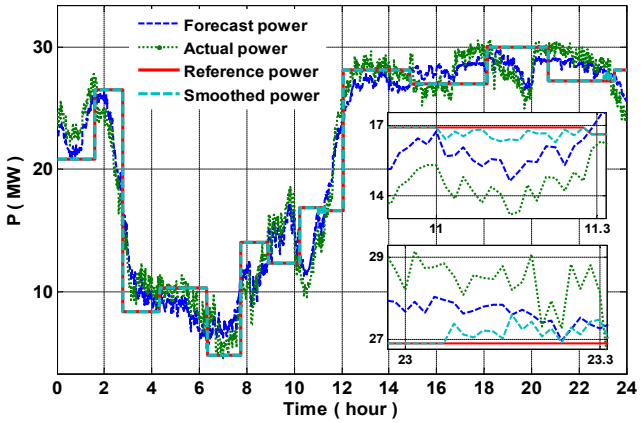

Fig.13 Performance of the fluctuation smoothing

Apparently, VRB can address the forecast error with a good performance. Specially, due to the limited size of VRB, between [11, 11.3] and [23, 23.3] hour minor deviations between reference power and the smoothed power occur. However, the smoothed wind power is still acceptable and the deviation also directly reflects the tradeoff between cost and performance.

E. Battery lifetime analysis

With the proposed control strategy, the average time interval of reference output can be prolonged and meanwhile over-discharge can be effectively constrained. Furthermore, if the lifetime of the size-limited BESS in this paper can be prolonged, the performance of the presented strategy can be further verified. According to (12), it should be noted that the battery lifetime has relationship with the reference wind power, which determines the charged/discharged energy in BESS. Accordingly, battery lifetime is analyzed with three different cases.

1) Case 1: Wind power is smoothed on an hourly basis, and BESS can deep discharge with no SOC limits.

2) Case 2: Wind power is smoothed on an hourly basis, and SOC is constrained within [0.15, 1.0]. Whenever SOC is below 0.25, it is treated as over-discharge and w_i^o will increase to be 1.5 to evaluate the damage of over-discharge.

3) Case 3: This case shows the presented cycle control strategy. Wind power is smoothed with flexible reference output, and over-discharge has been effectively constrained with flexible SOC ranges.

TABLE IV
BATTERY LIFETIME ANALYSIS

	Case 1	Case 2	Case 3
Reference output	Hourly	Hourly	Flexible
SOC ranges	[0,1]	[0.15,1]	Flexible
Over-discharge	Not constrained	Constrained	Avoided
E_{dev} (MWh)	4013	4771	769
Battery lifetime	0.89	0.96	1.0

In Table IV, battery lifetime is shown as per unit value of the lifetime of Case 3. It can be seen that the flexible reference and SOC ranges in Case 3 can avoid over-discharge effectively. Without SOC constraints, E_{dev} in Case 1 is smaller than Case 2, but it results in serious over-discharge which affects the battery lifetime apparently. Although the SOC limit in Case 2 constrains the over-discharge to some extent, the largest E_{dev} shows that the wind power in Case 2 cannot be effectively smoothed. Ignoring the performance of fluctuation smoothing, if only lifetimes are paid attention to, it can be seen the lifetimes in Case 2 and 3 are very close, while Case 1 has the shortest lifetime. The reason is mainly concerned with seasonal variation pattern of wind power. In winter, the dramatic fluctuations easily incur over-discharge in the hourly reference output to impact the BESS lifetime, while the fluctuation pattern has little influence on the presented strategy. Accordingly, due to the measures to constrain over-discharge in Case 2, its lifetime is longer than Case1and meanwhile close to Case 3.

VII. CONCLUSION

A novel optimal control and sizing scheme for BESS integrated with wind farm is proposed in this paper. The simulation based on actual wind power data validates the performance of the presented scheme. By decreasing the charge/discharge switch and avoiding over-discharge, the proposed control and sizing scheme can effectively protect BESS to prolong its lifetime. Besides, the time duration distribution shows that the reference outputs are more dispatch-able to benefit the wind power trading and the SOC curves demonstrate the promotion of BESS utilization. The real-time operation also verifies its excellent performance in dealing with the forecast error.

REFERENCES

[1] A. Sturt and G. Strbac, "Efficient stochastic scheduling for simulation of wind integrated power systems," *IEEE Trans. Power Syst.*, vol. 27, no. 1, pp. 323–334, Feb. 2012.

[2] F. Bouffard and F.D. Galiana, "Stochastic security for operations planning with significant wind power generation," *IEEE Trans. Power Syst*., vol. 23, no. 2, pp. 306–316, Apr. 2008.

[3] C. Wan, Z. Xu, P. Pinson, Z.Y. Dong, and K.P. Wong, "Probabilistic forecasting of wind power generation using extreme learning machine," *IEEE Trans. Power Syst.,* vol. 29, no. 3, pp. 1033–1044, May 2014.

[4] K. Meng, Z.Y. Dong, Y. Zheng, J. Qiu, and K.P. Wong, "Optimal allocation of ESS in distribution systems considering wind power uncertainties," *Adv. in Power Syst. Contr. Oper. Manag.*, Hong Kong, 2012.

[5] K.W. Wee, S.S. Choi and D.M. Vilathgamuwa, "Design of a least-cost battery super-capacitor energy storage system for realizing dispatch-able wind power," *IEEE Trans. Sustain. Energy*, vol. 4, no. 3, pp. 786–795, Jul. 2013.

[6] Q. Jiang, Y. Gong, and H. Wang, "A battery energy storage system dual-layer control strategy for mitigating wind farm fluctuations," *IEEE Trans. Power Syst*., vol. 28, no. 3, pp. 3263–3273, Aug. 2013.

[7] K. Zhang, C. Mao, J. Lu, et al, "Optimal control of stage-of-charge of superconducting magnetic energy storage for wind power system," *IET Renew. Power Gener.*, vol. 8, no. 1, pp. 58–66, Oct. 2014.

[8] F. Luo, K. Meng, Z.Y. Dong, Y. Zheng, Y. Chen and K.P. Wong. "Coordinated operational planning for wind farm with battery energy storage system," *IEEE Trans. Sustain. Energy*, vol. 6, no. 1, pp. 253–262, Jan. 2015.

[9] T.K.A. Brekken, A. Yokochi, A.e von Jouanne, and Z.Z. Yen, "Optimal energy storage sizing and control for wind power application," *IEEE Trans. Sustain. Energy*, vol. 2, no. 1, pp.69–77, Jan. 2011.

[10] S. Teleke, M.E. Baran, and S. Bhattacharya, "Optimal control of battery energy storage for wind farm dispatching," *IEEE Trans. Energy Convs.,* vol. 25, no. 3, pp. 787–794, Sep. 2010.

[11] H.T. Le, S. Santoso and T.Q. Nguyen, "Augmenting wind power penetration and grid voltage stability limits using ESS: application design, sizing, and a case Study," *IEEE Trans. Power Syst*., vol. 27, no. 1, pp. 161–171, Feb. 2012.
[12] Igor Papič, "Simulation model for discharging a lead-acid battery energy storage system for load leveling," *IEEE Trans. Energy Convs.,* vol. 21, no. 2, pp. 608–615, Jun. 2006.
[13] L. Xu, X.B. Ruan, C.X. Mao, and B.H. Zhang, "An improved optimal sizing method for wind-solar-battery hybrid power system," *IEEE Trans. Sustain. Energy*, vol. 4, no. 3, pp. 774–785, Jul. 2013.
[14] Y. Zheng, Z. Y. Dong, F.J. Luo *et al*., "Optimal allocation of energy storage system for risk mitigation of DISCOs with high renewable penetrations," *IEEE Trans. Power Syst.*, vol. 29, no. 1, pp. 212–220, Jan. 2014.
[15] S. Teleke, M.E. Baran, A.Q. Huang, S. Bhattacharya, and L. Anderson, "Control strategies for battery energy storage for wind farm dispatching," *IEEE Trans. Energy Convs.,* vol. 24, no. 3, pp. 725–732, Sep. 2009.
[16] S. Teleke, M. E. Baran, S. Bhattacharya, *et al.*, "Rule-based control of battery energy storage for dispatching intermittent renewable sources," *IEEE Trans. Sustain. Energy,* vol. 1, no. 3, pp. 117–124, Oct. 2010.
[17] D.L. Yao, S.S. Choi, K.J. Tseng, and T.T. Lie, "Determination of short-term power dispatch schedule for a wind farm incorporated with dual-battery energy storage scheme," *IEEE Trans. Sustain. Energy*, vol. 3, no. 1, pp. 74–84, Jan. 2012.
[18] G. N. Bathurst, J. Weatherill, and G. Strbac, "Trading wind generation in short term energy markets," *IEEE Trans. Power Syst.,* vol. 17, no. 3, pp. 782–789, Aug. 2002.
[19] H. Chen, T.N. Cong, W. Yang, C. Tan, Y. Li, and Y. Ding, "Progress in electrical energy storage system: A critical review," *Prog. Natural Sci.*, vol. 19, no. 3, pp. 291–312, Mar. 2009.
[20] "Lifetime modelling of lead acid batteries," Risø National Laboratory, Denmark, Apr. 2005.
[21] D. Tran and A.M. Khambadkone, "Energy management for lifetime extension of energy storage system in micro-grid application," *IEEE Trans. Smart Grid*, vol. 4, no. 3, pp.1289–1296, Sep. 2013.
[22] K. Deb, A. Pratap, S. Agarwal, and T. Meyarivan, "A fast elitist multi-objective genetic algorithm: NSGA-II," *IEEE Trans. Evol. Comput*, vol. 6, no. 2, pp. 182–197, Apr. 2002.
[23] X. Wang, M. Yue, E. Muljdi and W. Gao, "Probabilistic approach for power capacity specification of wind energy storage systems," *IEEE Trans. Indust. Appl*, vol. 50, no. 2, pp. 1215–1224, Apr. 2014.
[24] A. Damiano, G. Gatto, I. Marongiu, M. Porru and A. Serpi, "Real-time control strategy of energy storage systems for renewable energy sources exploitation," *IEEE Trans. Sustain. Energy*, vol. 5, no. 2, pp. 567–576, Apr. 2014.
[25] Q. Li, S.S. Choi, Y. Yuan, D.L. Yao, "On the determination of battery energy storage capacity and short-term power dispatch of a wind farm," *IEEE Trans. Sustain. Energy*, vol. 2, no. 2, pp. 148–158, Jan. 2011.
[26] Tu A. Nguyen, Mariesa L. Crow, and Andrew Curtis Elmore, "Optimal sizing of a vanadium redox battery system for microgrid systems," *IEEE Trans. Sustain. Energy*, vol.6, no. 3, pp.74–84, Jul. 2015.

Feng Zhang (M'11) received his Ph.D. degree from Shandong University, China, in 2011. He is currently with School of Electrical Engineering, Shandong University, Jinan, China. During 2015 and 2016, he was a Research Associate at the Department of Electrical Engineering, The Hong Kong Polytechnic University. He is now a visiting scholar in the University of Sydney. His research interest includes renewable energy, micro-grid, energy storage, and economic dispatch of power system.

Guibin Wang (M'16) received his B.E. and Ph.D. degrees in electrical engineering from Shandong University, Jinan, China and Zhejiang University, Hangzhou, China, in 2009 and 2014, respectively. During 2011-2012 and 2013-2014, he was a research assistant in the Department of Electrical Engineering, Hong Kong Polytechnic University, Hong Kong. He is now an assistant professor in Shenzhen University, Shenzhen, China. His main research interests lie in electric vehicles and renewable energy.

Ke Meng (M'10) obtained Ph.D. from the University of Queensland, Australia in 2009. He is currently with the School of Electrical and Information Engineering, The University of Sydney, Australia. Before that, he was a research academic with the center for intelligent electricity networks, the University of Newcastle, Australia. He is also a visiting Professor of the Changsha University of Science and Technology. His research interest includes pattern recognition, power system stability analysis, wind power, and energy storage.

Junhua Zhao (M'07) received his Ph.D. degree from the University of Queensland, Australia. Currently he is an Associate Professor at The Chinese University of Hong Kong (Shen Zhen), China. Before that, he was a Senior Lecturer at the Centre for Intelligent Electricity Networks (CIEN), The University of Newcastle, Australia. He is currently a National "1,000 Talents Program" Distinguished Young Scholar of China. His research interests include power system analysis and computation, smart grid, Energy Internet, electricity market, data mining, and artificial intelligence.

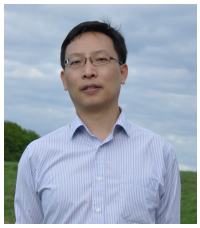

Zhao Xu (M'06-SM'13) received his B.Eng., M. Eng., and Ph.D. degrees from Zhejiang University, China, in 1996, National University of Singapore, Singapore, in 2002, and The University of Queensland, Australia, in 2006, respectively.

He is now with The Hong Kong Polytechnic University. He was previously with Centre for Electric Power and Energy, Technical University of Denmark. His research interest includes demand side, grid integration of renewable energies and EVs, electricity market planning and management, and AI applications in power engineering. He is an Editor of IEEE Transactions on Smart Grid, IEEE POWER ENGINEERING LETTERS, and Electric Power Components and Systems journal.

Zhao Yang Dong (M'99-SM'06-F'17) obtained his Ph.D. degree from the University of Sydney, Australia in 1999. He is now Professor and Head of School of Electrical and Information Engineering, University of Sydney, Australia. He was previously Ausgrid Chair and Director of the Center for Intelligent Electricity Networks (CIEN), The University of Newcastle, Australia, and is now a conjoint professor there. He also held academic and industrial positions with the Hong Kong Polytechnic University and Transend Networks (now TASNetworks), Tasmania, Australia. His research interest includes Smart Grid, power system planning, power system security, load modeling, electricity market, and computational intelligence and its application in power engineering. Prof. Dong is an editor of IEEE Transactions on Smart Grid, IEEE Transactions on Sustainable Energy, IEEE Power Engineering Letters, and IET Renewable Power Generation.

Jun Liang received his Ph.D. degree from the School of Electrical Engineering at Shandong University, Jinan, China. He is currently a Professor at Shandong University. His research interest includes power system analysis and operation, renewable energy, micro-grid and energy storage.